Speed of wave-front solutions to hyperbolic reaction-diffusion equations

Vicenç Méndez,[1] Joaquim Fort,[2] and Jordi Farjas[2]
[1]*Facultat de Ciències de la Salut, Universitat Internacional de Catalunya, Gomera s/n, 08190 Sant Cugat del Vallès, Barcelona, Catalonia, Spain*
[2]*Departament de Física, Escola Politècnica Superior, Universitat de Girona, Avenida Lluís Santaló s/n, 17071 Girona, Catalonia, Spain*
(Received 2 March 1999; revised manuscript received 21 July 1999)

The asymptotic speed problem of front solutions to hyperbolic reaction-diffusion (HRD) equations is studied in detail. We perform linear and variational analyses to obtain bounds for the speed. In contrast to what has been done in previous work, here we derive upper bounds in addition to lower ones in such a way that we can obtain improved bounds. For some functions it is possible to determine the speed without any uncertainty. This is also achieved for some systems of HRD (i.e., time-delayed Lotka-Volterra) equations that take into account the interaction among different species. An analytical analysis is performed for several systems of biological interest, and we find good agreement with the results of numerical simulations as well as with available observations for a system discussed recently. [S1063-651X(99)06211-X]

PACS number(s): 05.70.−a, 05.40.−a

I. INTRODUCTION

Reaction-diffusion equations have been used to describe very different processes in fluid dynamics, dendritic and population growth, pulse propagation in nerves, and many other biological, chemical, and physical phenomena. The ensuing equations are derived from the classical diffusion equation which, after taking into account a source (also called reaction) term $f(n)$, adopts the form $n_t = n_{xx} + f(n)$, where n is the density of particles and $f(n)$ is a nonlinear function with at least two equilibrium states. Equations of this kind are called parabolic reaction-diffusion (PRD) equations. It has been shown by Aronson and Weinberger [1] that sufficiently localized initial conditions evolve asymptotically into a traveling monotonic wave front connecting two equilibrium states. The asymptotic speed at which the front propagates is the minimal speed c for which there is a monotonic front joining both states. Some solutions to reaction-diffusion equations seem to be particularly important to describe the dynamics of such systems, namely the so-called wave-front solutions. Wave fronts are solutions of constant speed connecting equilibrium states, namely the roots of $f(n)$. It is observed both experimentally and numerically that the global, nonlinear dynamics rapidly selects a unique solution. The speed at which the front moves towards the stable state is referred to as the selected speed. There already exist several proposed criteria in the literature for the analysis of the dynamical velocity selection: a minimum speed rule [2], structural stability [3], marginal stability [2,4], and many others. The marginal stability approach was studied initially by Dee and Langer [2] and Ben-Jacob *et al.* [4]. According to the marginal stability hypothesis, for most sufficiently localized initial conditions, the propagation velocity of well-developed fronts generically approaches the marginal-stability point which apparently coincides with the minimal velocity. This point may be calculated explicitly from the linearized leading-edge approximation, in which only the linearized equation of motion is studied near the front. In the literature, this is sometimes referred to as the linear-marginal-stability case. All of this work refers, however, to parabolic reaction-diffusion (PRD) equations.

An important feature of diffusive phenomena is the existence of a delay time [5–7]. In reactive systems, this can be taken into account by resorting to hyperbolic reaction-diffusion (HRD) equations, which generalize PRD equations. The existence of wave fronts in HRD equations has been analyzed by Hadeler [8] and has been recently applied to population growth [9], forest fire models [10], bistable systems [11], and the Neolithic transition [12]. A rather complete study of the wave-front speed problem in HRD equations is the aim of this work.

Our starting point is a system of reacting particles, following one-dimensional equations for the time evolution of the number density n and flux J of particles

$$\frac{\partial n}{\partial t} + \frac{\partial J}{\partial x} = F(n), \tag{1}$$

$$\tau \frac{\partial J}{\partial t} + J = -D \frac{\partial n}{\partial x}, \tag{2}$$

where the first equation is the balance equation for n and the second one is the transport equation for the flux J. For microscopic derivations of Eqs. (1) and (2), see Refs. [9] and [12]. $F(n)$ is the source function corresponding to the reactive process, D is the diffusion coefficient, and τ is the relaxation (or delay) time. When $F(n)=0$ the systems (1) and (2) reduce to the telegrapher's equation of diffusion [7], whereas for $\tau=0$ we have the classical, PRD description of reaction diffusion (see, e.g., Ref. [1]).

II. LINEAR ANALYSIS

From Eqs. (1) and (2) it is easy to obtain the so-called HRD equation,

$$\tau n_{tt} + n_t = D n_{xx} + F(n) + \tau F'(n) n_t . \tag{3}$$

Here τ is the mean collision time for chemical reactions [12], [13], time between two consecutive generations in human migrations [12], mean ignition time in forest fire models [10], etc., and the primed symbol denotes $'=d/dn$. It is convenient to rescale Eq. (3) for further purposes as follows:

$$t^*=kt,$$

$$x^*=x\sqrt{k/D},$$

and write $F(n)=kf(n)$, where $1/k$ is a characteristic time of the reactive process. We define $a=k\tau$. Then Eq. (3) becomes, omitting asterisks for notational simplicity,

$$an_{tt}+n_t=n_{xx}+f(n)+af'(n)n_t. \tag{4}$$

In the absence of a delay time ($\tau=0$), this reduces to the classical (or PRD) equation $n_t=n_{xx}+f(n)$, which has been recalled in Sec. I. For simplicity we will consider reaction terms $f>0$ which vanish at $n=0$ and $n=1$. It has been shown [8] that Eq. (4) has traveling wave fronts with profile $n(x-ct)$ and moving with speed $c>0$, which will satisfy the equation

$$(1-ac^2)n_{zz}+c[1-af'(n)]n_z+f(n)=0, \tag{5}$$

where $z=x-ct$, and with boundary conditions $\lim_{z\to\infty}n=0$, $\lim_{z\to-\infty}n=1$, and $n_z<0$ in (0,1); n_z vanishes for $z\to\pm\infty$ [8]. We will now analyze how linear stability analysis can be applied to HRD equations, in order to study the speed of the front.

Linear analysis makes it possible to study the behavior of the wave front near the equilibrium states, which according to Eq. (1) are the solutions to the equation $f(n)=0$, say $n=0$ and $n=1$. In Ref. [9] the lower bound $c>2\sqrt{f'(0)}/[1+af'(0)]$ was derived by analyzing the trajectories in the phase space (n,n_z). Here we will summarize an alternative approach that yields the same conditions on the front velocity but, in contrast to the one in Ref. [9], it will allow us to analyze the asymptotic behavior of $n(z)$ near the equilibrium points. This behavior will in turn be used in the derivation of better bounds on the speed in the next section.

A. $n\approx 0$

Setting $\epsilon(z)=n(z)\ll 1$, we linearize Eq. (5) to obtain the front equation near $n=0$. We get

$$(1-ac^2)\epsilon_{zz}+c[1-af'(0)]\epsilon_z+f'(0)\epsilon=0. \tag{6}$$

Solutions of the form $\epsilon\sim e^{\lambda z}$ provide us with the following characteristic equation:

$$(1-ac^2)\lambda^2+c[1-af'(0)]\lambda+f'(0)=0. \tag{7}$$

So, the solution of the linearized equation (6) near $n=0$ is given by

$$\epsilon(z)=A_+e^{\lambda_+ z}+A_-e^{\lambda_- z}, \tag{8}$$

where A_+ and A_- are integration constants (depending on the initial and boundary conditions) and $\lambda_\pm$ are the solutions of the characteristic equation (7). Since $\epsilon(z)=n(z)$ is the number density of particles, it cannot be negative for any possible value of z, thus $\lambda_\pm\in\mathbb{R}$. It therefore follows from Eq. (7) that

$$c\geqslant c_L=\frac{2\sqrt{f'(0)}}{1+af'(0)}, \tag{9}$$

where it has been assumed that $f'(0)>0$. If this does not hold, the approach we shall present in this section breaks down. This happens, e.g., in forest fire models (discussed in Sec. IV D in the present paper), and in such cases one may resort the variational analysis we will develop in Sec. III.

In the limit $z\to+\infty$ one has $n\to 0$ as boundary condition, so $\lambda_\pm$ must be negative. If one (or both) values of λ were positive, then in the limit $z\to+\infty$ one would have $n\to+\infty$ and we would not be dealing with a solution connecting the equilibrium states $n=1$ and $n=0$, thus the solution under consideration would not satisfy the definition of a wave front, given in Sec. I. Therefore, Eq. (7) yields the conditions

$$c<1/\sqrt{a}, \tag{10}$$

$$1-af'(0)>0. \tag{11}$$

B. $n\approx 1$

We now introduce $\epsilon(z)=1-n(z)>0$ and $f(n)\simeq -f'(1)(1-n)=|f'(1)|\epsilon$, assuming $f'(1)<0$ (this is necessary in order to avoid an unbounded population growth in biological applications [14]). The linearized Eq. (5) near $n=1$ is

$$(1-ac^2)\epsilon_{zz}+c[1+a|f'(1)|]\epsilon_z-|f'(1)|\epsilon=0. \tag{12}$$

This equation holds for $n\approx 1$ and is the analog to Eq. (6), which holds for $n\approx 0$. Similarly, for $n\approx 1$ Eqs. (7) and (8) are replaced by

$$(1-ac^2)\lambda^2+c[1+a|f'(1)|]\lambda-|f'(1)|=0, \tag{13}$$

$$\epsilon(z)=B_+e^{\lambda_+ z}+B_-e^{\lambda_- z}, \tag{14}$$

respectively. Here we note that there are real two solutions for λ, one of them being positive (say λ_+) and the other one negative (say λ_-). Thus, contrary to what happened in the case $n\approx 0$ (where λ_+ and λ_- could both be required to be negative in order to ensure that $n\to 0$ for $z\to\infty$ for arbitrary initial conditions), here we have $\lambda_+>0$ and $\lambda_-<0$. Now since we must require that $n\to 1$ for $z\to-\infty$, we see that it is necessary that $B_-=0$, i.e., for $n\approx 1$ only $\lambda_+>0$ will appear in the asymptotic solution (14), whereas for $n\approx 0$ both $\lambda_+<0$ and $\lambda_-<0$ appear in the corresponding solution (8). This general result is reached here and is in agreement with an explicit solution, which was derived previously for a very specific source term $f(n)$ and initial condition (see Sec. V in Ref. [9]).

Just to summarize, the linear analysis presented in this section shows the existence of a traveling wave front, connecting the equilibrium states $n=0$ and $n=1$, provided that the front satisfies the conditions (9), (10), and (11).

The marginal-stability analysis (MSA), performed by van Saarloos for PRD equations [15], may also be applied to

HRD equations. It is possible to show that the linear approach we have presented and the corresponding MSA yield the same result (9). Thus we will not develop the MSA for HRD equations explicitly. Let us mention, however, that there are thin differences between both analyses. In MSA one does not assume uniformly translating fronts of the form $n(x-ct)$ but the procedure is more general and refers to the velocity of the envelope. The present paper is devoted to Eq. (3), which is a HRD equation that does not yield states behind the front that are periodic in space. In the case of equations that lead to periodic states, a uniformly translating front cannot occur, so that it would be necessary to investigate the envelope of the front by means of the MSA.

III. VARIATIONAL ANALYSIS

In this section we follow the variational analysis by Benguria and Depassier for PRD equations [16]. We will extend it to HRD equations. We start from Eq. (5) and define $p(n)=-n_z$ with $p(0)=p(1)=0$ and $p>0$ in (0,1). Equation (5) may be written as

$$(1-ac^2)p\frac{dp}{dn}-c[1-af'(n)]p+f(n)=0. \tag{15}$$

Let $g(n)$ be an arbitrary positive function; multiplying Eq. (15) by g/p and integrating by parts we obtain

$$c\int_0^1 g[1-af'(n)]dn=\int_0^1\left[(1-ac^2)hp+\frac{gf}{p}\right]dn, \tag{16}$$

where $h=-g'>0$ as chosen for PRD equations [17]. Now for any positive numbers r and s, it follows from $(r-s)^2$ that $(r+s)\geqslant 2\sqrt{rs}$. If $1-ac^2>0$ or $c<1/\sqrt{a}$, since f, g, h, and p are positive, we may choose $r\equiv(1-ac^2)hp$ and $s\equiv gf/p$ to get a restriction on c which eliminates p,

$$(1-ac^2)hp+\frac{gf}{p}\geqslant 2\sqrt{1-ac^2}\sqrt{fgh}, \tag{17}$$

and therefore,

$$\frac{c}{\sqrt{1-ac^2}}\geqslant 2\frac{\int_0^1\sqrt{fgh}dn}{\int_0^1 g[1-af'(n)]dn}. \tag{18}$$

If the effect of the delay time τ is neglected (i.e., for $a=k\tau\approx 0$), this reduces to the Benguria-Depassier principle [16,17]. To see that Eq. (18) is a variational principle we must show that there is a function $g=\hat{g}$ for which the equality holds. From the explanation above Eq. (17) we see that this happens when $r=s$ or $(1-ac^2)\hat{h}p=\hat{g}f/p$, which according to our HRD equation (15) implies that $\hat{g}$ satisfies the ordinary differential equation

$$\frac{\hat{g}'}{\hat{g}}=-\frac{c}{1-ac^2}\frac{1-af'(n)}{p}+\frac{p'}{p}.$$

The corresponding $\hat{g}$, obtained by integrating this equation, is given by

$$\hat{g}(n)\sim p(n)\exp\left[-\frac{c}{1-ac^2}\int_{n_0}^{n}\frac{1-af'(\tilde{n})}{p}d\tilde{n}\right] \tag{19}$$

with $0<n_0<1$. Evidently $\hat{g}(n)$ is a continuous positive function. We will now determine the behavior of $\hat{g}(n)$ near $n=0$ and see that the integrals in Eq. (18) exist. To verify this we recall, from the linear analysis, that the front approaches $n=0$ exponentially. From this, it is easily seen that the dominant term in Eq. (8) yields $p=-dn/dz\sim\mu n$, where

$$\mu=\frac{1}{2(1-ac^2)}[c[1-af'(0)]+\sqrt{c^2[1+af'(0)]^2-4f'(0)}].$$

For $\tau=0$ this reduces, as it should, to the result derived for PRD equations by Aronson and Weinberger [1] (see also Ref. [17]). Thus, from Eq. (19) we get, near $n=0$,

$$\hat{g}(n)\sim n^{1-\gamma},$$

where

$$\gamma=\frac{c[1-af'(0)]}{\mu(1-ac^2)}.$$

We also get in this limit $\sqrt{f\hat{g}\hat{h}}\sim\hat{g}f'(n)\sim n^{1-\gamma}$. Hence the integrals in Eq. (18) exist if $\gamma<2$. This condition is satisfied provided that $c>2\sqrt{f'(0)}/[1+af'(0)]$, which is in agreement with the condition (9) derived form the linearization method.

Therefore, we have shown that the asymptotic speed of the front is given by

$$\frac{c}{\sqrt{1-ac^2}}=\max_g\left(2\frac{\int_0^1\sqrt{fgh}dn}{\int_0^1 g[1-af'(n)]dn}\right). \tag{20}$$

It is important to notice that the variational result given by Eq. (20) requires two strong conditions, in order to be applicable, namely $c<1/\sqrt{a}$ and $1-af'(n)>0$. The second restriction is equivalent to $a<1/M$, with $M=\max_{n\in(0,1)}f'(n)$, and will be used explicitly in the derivation of upper bounds for the front velocity (Sec. III B below). In the following two subsections we analyze whether the variational result leads to lower and upper bounds for the asymptotic speed and compare to the results from the linear analysis (Sec. II). We will show that the linear (and marginal) stability value for the speed c_L Eq. (9) also follows from the variational expression (18). More importantly, we shall also show that the variational result (20) makes it possible to obtain a better upper bound on the speed than that following from linear stability, i.e., $c<c_{\max}=1/\sqrt{a}$ [see Eq. (10)].

A. Lower bounds

As we have mentioned in the study above, one may obtain a lower bound for the asymptotic speed, by means of a given function $g(n)$. This trial function must satisfy that $g(n)>0$ and $g'(n)<0$ in (0,1). Consider the simple sequence of trial functions $g=n^{\alpha-1}$ in the limit $\alpha\to 0$. These functions are positive and have negative derivative for $0\leqslant\alpha<1$, as required in the derivations above. According to Eq. (18) or (20),

$$\frac{c}{\sqrt{1-ac^2}}\geqslant 2\sqrt{1-\alpha}\,\frac{\int_0^1 n^{\alpha-3/2}\sqrt{f(n)}dn}{\int_0^1 n^{\alpha-1}[1-af'(n)]dn}.$$

In the limit $\alpha\to 0$, the integrands diverge at $n=0$, as in the case of PRD equations [16], thus only the singular point will contribute in the limit. The surviving contributions are then

$$\frac{c}{\sqrt{1-ac^2}}\geqslant 2\sqrt{1-\alpha}\,\frac{\int_0^\varepsilon n^{\alpha-3/2}\sqrt{f(n)}dn}{\int_0^\varepsilon n^{\alpha-1}[1-af'(n)]dn}.$$

We may expand the integrands in Taylor series near $n=0$. Only the leading term in the expansions will contribute as $\alpha\to 0$ and we have, assuming $f'(0)\neq 0$,

$$\frac{c}{\sqrt{1-ac^2}}\geqslant 2\sqrt{1-\alpha}\,\frac{\int_0^\varepsilon n^{\alpha-3/2}\sqrt{f'(0)n}dn}{\int_0^\varepsilon n^{\alpha-1}[1-af'(0)]dn}.$$

Performing the integrals and taking the limit $\alpha\to 0$ we obtain

$$\frac{c}{\sqrt{1-ac^2}}\geqslant\frac{2\sqrt{f'(0)}}{1-af'(0)},\tag{21}$$

thus

$$c\geqslant c_L=\frac{2\sqrt{f'(0)}}{1+af'(0)}.\tag{22}$$

This reduces, as it should, to the classical or PRD value $c_L=2\sqrt{f'(0)}$ [1] if the effect of the delay time is neglected ($a\approx 0$). It is seen that the lower bound (22) is the same as Eq. (9), which is also known from the derivation of the variational principle above. We conclude that the variational principle we have derived does not provide better lower bounds for the speed of wave fronts than the linear or MSA approaches if we choose $g(n)=n^{\alpha-1}$. As we shall see in detail in the following subsection, the opposite happens for upper bounds. Moreover, the method presented above for $g(n)=n^{\alpha-1}$ is of interest since it does yield better lower bounds for other trial functions $g(n)$, depending on the source function considered (an explicit example will be presented in Sec. IV D).

B. Upper bounds

Here we derive upper bounds for the asymptotic speed by extending to HRD equations the recent development by Benguria and Depassier [16]. We need the particular case of Jensen's inequality [18]

$$\frac{\int_0^1\mu(n)\sqrt{\alpha(n)}dn}{\int_0^1\mu(n)dn}\leqslant\sqrt{\frac{\int_0^1\mu(n)\alpha(n)dn}{\int_0^1\mu(n)dn}},\tag{23}$$

where $\mu(n)>0$ and $\alpha(n)\geqslant 0$. If we define $\mu(n)=g(n)[1-af'(n)]$ and $\alpha(n)=f(n)h(n)/\{g(n)[1-af'(n)]^2\}$, then the left-hand side of the above inequality may be written as

$$\frac{\int_0^1\mu(n)\sqrt{\alpha(n)}dn}{\int_0^1\mu(n)dn}=\frac{\int_0^1\sqrt{fgh}dn}{\int_0^1 g(1-af')dn},$$

and inside the square root in the right-hand side we have

$$\frac{\int_0^1\mu(n)\alpha(n)dn}{\int_0^1\mu(n)dn}=\frac{\int_0^1\frac{fh}{1-af'}dn}{\int_0^1 g(1-af')dn}.$$

We have then, from Eqs. (20) and (23), a relatively simple expression which will allow us to find upper bounds

$$\frac{c}{\sqrt{1-ac^2}}=2\max_g\left(\frac{\int_0^1\sqrt{fgh}dn}{\int_0^1 g(1-af')dn}\right)\leqslant 2\max_g\left[\frac{\int_0^1\frac{fh}{1-af'}dn}{\int_0^1 g(1-af')dn}\right]^{1/2}.\tag{24}$$

We now observe that integration by parts makes it possible to find an expression in which $h=g'$ no longer appears,

$$\int_0^1\frac{fh}{1-af'}dn=\int_0^1 g\,\frac{f'+a(ff''-f'^2)}{(1-af')^2}dn.\tag{25}$$

Moreover, in order to get an upper bound independent of g, we write Eq. (25) in a more useful form,

$$\int_0^1\frac{fh}{1-af'}dn=\int_0^1 g(1-af')\frac{f'+a(ff''-f'^2)}{(1-af')^3}dn\leqslant\sup_{n\in(0,1)}\left[\frac{f'+a(ff''-f'^2)}{(1-af')^3}\right]\int_0^1 g(1-af')dn,\tag{26}$$

were we have applied the condition $(1-af')>0$. Finally,

$$\frac{c}{\sqrt{1-ac^2}} \leqslant 2\sqrt{\sup_{n\in(0,1)} \Phi(n)} \tag{27}$$

where

$$\Phi(n) \equiv \frac{f' + a(ff'' - f'^2)}{(1-af')^3}. \tag{28}$$

Hence the upper bound may be written as

$$c_U = \frac{2q(a)}{\sqrt{1+4aq^2(a)}}, \tag{29}$$

where $q(a) = \sqrt{\sup_{n\in(0,1)}\Phi(n)}$. This result may be written in a simpler form if we assume that the source function $f(n)$ is continuous and concave, i.e., $f'' < 0$, in (0,1). Then, since $f(0) = f(1) = 0$ we have $f'(0) > 0$ and $f'(1) < 0$. We may write

$$\Phi(n) = \frac{f'}{(1-af')^2} + a\frac{ff''}{(1-af')^3},$$

where, recalling the condition $1 - af'(n) > 0$, we see that the second term is negative (it only vanishes at $n = 0,1$). Moreover, since we have assumed that f is continuous and that $f'' < 0$, the first term decreases for increasing values of n. Thus,

$$\sup_{n\in(0,1)} \Phi(n) = \frac{f'(0)}{[1-af'(0)]^2},$$

and we have the simpler result

$$c \leqslant c_U = \frac{2\sqrt{f'(0)}}{1+af'(0)}, \tag{30}$$

which holds provided that f is continuous and concave in (0,1). Some examples are discussed in Sec. IV. To the best of our knowledge, these results are the first ones for upper bounds in HRD equations. We note that the lower and upper bounds are the same [see Eq. (22)], so the asymptotic speed may be predicted without uncertainty. This generalizes the corresponding theorem for PRD equations ($a = 0$), which states that $c = 2\sqrt{f'(0)}$ provided that $f(n)$ is continuous and concave [1,17,19].

IV. APPLICATIONS

PRD equations have been studied for more than 60 years [20]. During this time, many important applications have been found, including the spread of advantageous genes [20,21], population dynamics [21,22], the development of epidemics [23], nerve conduction [24], models of mithocondrial tissue [25], cellular sensitivity [26], and other biological phenomena, in addition to physical applications such as superconductors [27], solidification [28], liquid crystals [29] and chemically reacting systems [30]. HRD equations have a comparatively much shorter history [8] and, as happened in the first applications of PRD equations, have for the moment been applied essentially to biological processes. This is reasonable since the value of the delay time in Eq. (2) is difficult to estimate in most physical systems: even for monatomic gases, Eq. (2) provides a very rough approximation since additional, higher-order terms are usually of the same order of magnitude as that in which τ appears, and it is necessary to take an infinite number of such terms and renormalize the corresponding expressions under suitable assumptions [31]. In this section we apply our results to a variety of source functions that are useful in the description of some interesting biological phenomena.

A. Logistic growth

Logistic growth has been used in hyperbolic reaction-diffusion equations to describe the dynamical and thermodynamical properties of delayed population growth [9]. Very recently, logistic growth in HRD equations has also been applied to the study of human migrations in the Neolithic transition [12]. The logistic source term is $f(n) = n(1-n)$, which is a realistic function driving the reproduction of many biological species [14]. This function satisfies the condition $f'(0) \neq 0$, is continuous and has $f'' < 0$. Whereas the linear analysis (Sec. I) gives only the lower bound (9), the variational results (22) and (30) show that the speed of the fronts is

$$c = \frac{2}{1+a}. \tag{31}$$

This result is in agreement with the recent work by Fedotov, which is based on the path-integral approach, the scaling procedure and singular perturbation techniques involving large deviation theory [32]. The result (31) is rather important in the context of the Neolithic transition, for in Ref. [12] we obtained good agreement with observations assuming that $c = 2/(1+a)$ is not just a lower bound but the actual speed of the population wave of the advance. If the effect of the delay time is neglected ($a = \tau k = 0$), we recover the well-known result $c = 2$ [20,1], which is the basis of the classical (or PRD) theory of the Neolithic transition [21]. Section V B in the present paper contains a refined model of the Neolithic transition.

We have solved Eq. (4) numerically for the logistic source function in order to determine the speed of the fronts for different values of a. The results of the simulations are compared to the analytical expression $c = 2/(1+a)$ in Fig. 1. The numerical simulations of Eq. (4) have been performed by assuming that initially $n = 1$ in a localized region and $n = 0$ elsewhere, and making use of the splitting operator technique [33]. The profile $n(x)$ was plotted at different times, and this has allowed us to determine the asymptotic speed selected by the smooth front that is observed after an initial transient. As far as we know, Fig. 1 presents the first simulations of hyperbolic wave fronts, and one may observe a rather satisfactory agreement between the numerical results and Eq. (31).

B. Generalized Fisher-Kolmogorov kinetics

The logistic function is the simplest one leading to some reasonable results such as the saturation of populations with

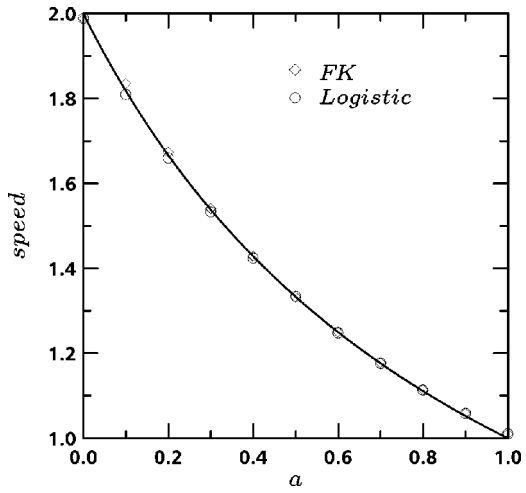

FIG. 1. Comparative plot between the analytical expression for the dimensionless speed $c=2/(1+a)$ and the dimensionless speed obtained from numerical integration of Eq. (4) as a function of the dimensionless parameter a for logistic growth (circles) and generalized FK kinetics, $p=2$ (rhombs). There is good agreement between numerical and analytical results.

a limited amount of available resources [14]. However, other source functions are important in biological applications. A particularly relevant case is the Fisher-Kolmogorov (FK) source function, namely $f(n)=n(1-n^2)$, which is important in genetics [20,19]. Here we will assume a generalized Fisher-Kolmogorov function,

$$f(n)=n(1-n^p),$$

with $p\geqslant 1$. As in the logistic case, we have $f'(0)\neq 0$, f is continuous and $f''<0$. Thus using the variational results (22) and (30) we can predict the speed of wave fronts without any uncertainty, $c=2/(1+a)$. It means that this result for the selected speed holds not only for the logistic case but also for more general situations of practical interest. From Fig. 1, we see that this prediction agrees with the simulations of Eq. (4) for the FK source function ($p=2$). We have also checked that there is good agreement for other values of p.

C. HRD generalization of a cubic PRD model

Consider next the cubic source function

$$f(n)=\frac{n}{b}(1-n)(b+n) \tag{32}$$

with $0<b<1$. This function has been applied in several reaction-diffusion studies on genetics, among them in the description of inferior heterozygotes selection [34] and of the morphogenetic field of a multicellular ensemble [35]. The source function (32) has also been useful because it can be solved exactly when the delay time is not accounted for ($a=0$) [4,17].

A lower bound for the speed of the fronts can be obtained from Eq. (9) or Eq. (22), namely $2/(1+a)$. On the other hand, the source term (32) is a concave function for $(1-b)/3<n<1$ and a convex function for $0<n<(1-b)/3$, so the upper bound (31) cannot be applied and we cannot obtain the exact asymptotic speed. However, we shall see that it is possible to constrain the speed. Let us first obtain a better lower bound. As in the case of PRD equations with the source term (32) [17], we choose $g(n)=(1-n)^{2+2b}n^{-2b}$. We now apply the method in Sec. III A for this single trial function instead of the sequence $g(n)=n^{\alpha-1}$. Equation (20) yields, after some algebra,

$$\frac{c}{\sqrt{1-ac^2}} \geqslant 2\frac{\frac{\sqrt{2b}}{\Gamma(4)}+\sqrt{\frac{2}{b}}\frac{1-2b}{\Gamma(5)}}{\frac{1-a}{\Gamma(4)}+\frac{6a}{b}\frac{(1-b)(1-2b)}{\Gamma(6)}-\frac{2a}{b}\frac{(1-b)(1-2b)}{\Gamma(5)}},$$

where the integrals have been solved making use of formula (3.191-3) in Ref. [18], which applies under the assumption that $0<b<1/2-$, $\Gamma(z)$ is the gamma function and we have applied that $\Gamma(z+1)=z\Gamma(z)$. From this we find the lower bound

$$c_L=\begin{cases} c_L(a,b), & 0<b<1/2 \\ \dfrac{2}{1+a}, & 1/2<b<1, \end{cases}$$

where

$$c_L(a,b)=\frac{\sqrt{2b}+1/\sqrt{2b}}{\sqrt{\left(1-\frac{a}{5}\frac{1+2b+2b^2}{b}\right)^2+\frac{a}{2b}(1+2b)^2}}.$$

Notice that for $1/2<b<1$ the integrals in Eq. (20) diverge, so that we have resorted to the lower bound (9) or (22). In the PRD case ($a=0$), we recover the result found by Ben-Jacob, namely $c_L=\sqrt{2b}+1/\sqrt{2b}$ for $0<b<1/2$ and $2/(1+a)$ for $1/2<b<1$ [4]. For the upper bound we cannot apply Eq. (30), as explained above, but we can still derive an upper bound from Eqs. (28) and (32). Equation (28) yields, after some algebra,

$$\Phi(n)=\frac{1+\frac{2}{b}n-2n-\frac{3}{b}n^2-a\left[1+\frac{2(1-b)}{b}n+\frac{2(1-2b+b^2)}{b^2}n^2-\frac{4(1-b)}{b^2}n^3-\frac{3}{b^2}n^4\right]}{\left[1-a\left(1+\frac{2}{b}n-2n-\frac{3}{b}n^2\right)\right]^3}$$

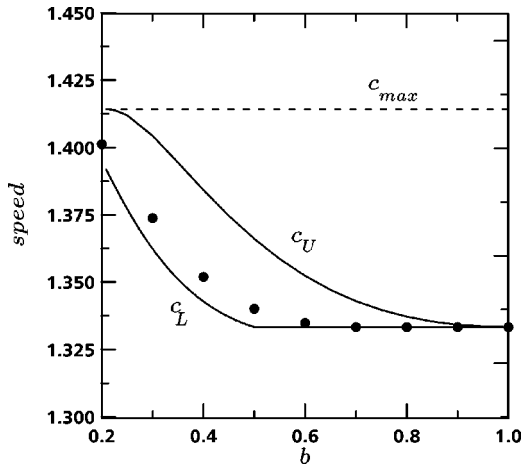

FIG. 2. Comparative plot between lower and upper bounds and the results from simulations of Eq. (4) for the cubic source function (32). Here $a=1/2$, and the range of values of b is constrained because of the range of validity of the variational approach. Lower and upper bounds are plotted in solid lines and numerical results in circles.

and the speed is given by Eq. (29). In the limit $b\to 1$, $f(n)$ is a concave function and $\sup \Phi(n)=\Phi(0)$, thus $c_U\to 2/(1+a)$. The variational analysis for the lower and upper bounds is restricted to the condition $1-af'>0$, which is equivalent to $a<M^{-1}$, with $M=\max_{n\in(0,1)}f'(n)$. For this case one finds $M=(1+b+b^2)/3b$ and the restriction is $(5-\sqrt{21})/2<b<1$ if $a=1/2$. We have plotted the bounds for $a=1/2$ in Fig. 2, as well as the results from numerical simulations of Eq. (4) with the source function (32), as a function of b. We observe good agreement between the simulations and the lower and upper bounds.

D. Forest fire models

HRD equations have been used to model the propagation of forest fires [10]. In this model a reaction term of the form

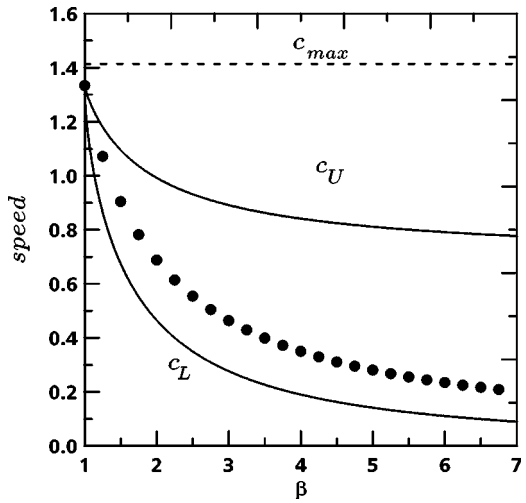

FIG. 3. Comparative plot between lower and upper dimensionless bounds and the numerical integration of Eq. (4) for the dimensionless speed of fire fronts as a function of parameter β, with $a=1/2$. The numerical values for the speed lie between both curves, as they should. As it is expected for forest fire models, the speed is a decreasing function for increasing values of β.

$$f(n)=n^{\beta}(1-n)$$

has been used. For $\beta=1$, this reduces to the logistic case dealt with in Sec. IV A, so we will assume that $\beta>1$. The parameter β quantifies the number of burning trees needed in order to set fire to a nearby, green tree. For high values of β, it is expected intuitively that the speed of the fire front will be smaller. Here we have $f'(0)=0$, thus the linear analysis does not hold. Therefore, we resort to the variational analysis. Still, since $f'(0)=0$, Eq. (22) does not apply, and since $f''<0$ does not hold everywhere in (0,1) Eq. (30) cannot be applied either. As in Sec. III A, let us consider the simple sequence of trial functions $g=n^{\alpha-1}$, with $0\leqslant\alpha<1$. The integrals in Eq. (20) are

$$\int_0^1 \sqrt{fgh}dn=\sqrt{1-\alpha}\,\frac{\Gamma\left(\frac{\beta}{2}+\alpha-\frac{1}{2}\right)\Gamma(3/2)}{\Gamma\left(\alpha+1+\frac{\beta}{2}\right)},$$

$$\int_0^1 g(1-af')dn=\frac{1}{\alpha}-a\,\frac{1-\alpha}{(\beta+\alpha)(\beta-1+\alpha)}.$$

Thus the best lower bound is given by

$$\frac{c_L}{\sqrt{1-ac_L^2}}=\max_{\alpha\in(0,1)}\{G(\alpha,\beta)\},$$

where

$$G(\alpha,\beta)=\frac{2\alpha\sqrt{1-\alpha}\,\Gamma\left(\frac{\beta}{2}+\alpha-\frac{1}{2}\right)\Gamma(3/2)}{\Gamma\left(\alpha+1+\frac{\beta}{2}\right)\left[1-a\,\frac{(1-\alpha)\alpha}{(\beta+\alpha)(\beta-1+\alpha)}\right]}.$$

We have calculated the value of α which maximizes $G(\alpha,\beta)$ numerically for $a=1/2$ and for different values of β between 1 and 7. The corresponding results for the lower bound c_L are plotted in Fig. 3.

For the upper bound we have to consider the function $\Phi(n)$, see Eq. (28). It reads

$$\Phi(n)=n^{\beta-2}\,\frac{\beta n-(\beta+1)n^2-an^{\beta}[\beta+(\beta+1)n^2-2\beta n]}{(1-a[\beta n^{\beta-1}-(\beta+1)n^{\beta}])^3}.$$

We set, as for the lower bound, $a=1/2$ and find the value n^* at which $\sup_{n\in(0,1)}\Phi(n)=\Phi(n^*)$ for different values of β between 1 and 7. For high values of β, $\Phi(n^*)$ must be computed numerically. The upper bound may be calculated finally from Eq. (27) or Eq. (29),

$$\frac{c_U}{\sqrt{1-ac_U^2}}=2\sqrt{\Phi(n^*)}.$$

The results for the upper bound are plotted, together with the lower bounds and the numerical solution for the speed, in Fig. 3 for $a=1/2$. The numerical solution is seen to lie between the upper and lower bounds, as it should, and it is a decreasing function with increasing values of β, as expected.

One could certainly try other trial functions $g(n)$ and find other bounds. We have used the same trial functions as in Sec. III A since they yield relatively simple results which illustrate fairly well the usefulness of the new variational principle here derived. It is also seen from Fig. 3 that the new upper bound c_U derived here is much better than $c_{\max}=1/\sqrt{a}=\sqrt{2}$ [see Eq. (10)], which had been derived previously [9].

E. Bistable systems

In several problems arising in biology (such as nerve conduction [36]), physics (electrothermal instability [37]), and chemistry (kinetic of bimolecular reactions [38,39]) it is found that the source term is given by

$$f(n)=n(1-n)(n-\sigma) \quad \text{for} \quad 0<\sigma<1. \tag{33}$$

In these cases the system is called bistable. The reason is the following: the parameter σ has a critical value $\sigma=1/2$ for which the stability of the states $n=0,1$ is inverted and the front changes its direction of propagation. For $\sigma<1/2$ the front connects $n=0$ to $n=1$ and $c>0$, for $\sigma=1/2$ we have $c=0$ and finally, for $1/2<\sigma<1$ the front connects $n=1$ to $n=0$ and $c<0$. This can be seen in Fig. 4. We look for bounds for the speed. We use the trial function $g(n)=(1-n)^{2-2\sigma}n^{2\sigma}$, as in the cubic HRD model (Sec. IV C). By following the same steps as in Sec. IV C, we now obtain the following lower bound:

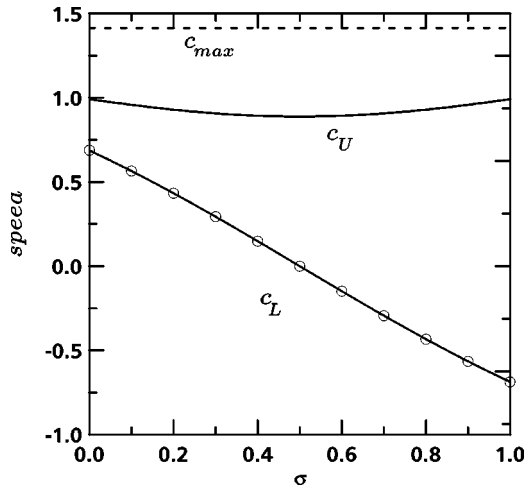

FIG. 4. Comparative plot between lower and upper bounds and the numerical solution for the dimensionless speed of fronts in bistable systems [Eq. (33)], for $a=1/2$. Note the change of sign for the speed at $\sigma=1/2$.

$$c_L=\frac{1-2\sigma}{\sqrt{2\left[1-\frac{a}{5}(1-2\sigma+2\sigma^2)\right]^2+a(1-2\sigma)^2}},$$

which holds for any $\sigma\in(0,1)$. Equation (28) yields, after some algebra,

$$\Phi(n)=\frac{-\sigma+2n(1+\sigma)-3n^2-a[-3n^4+4n^3(1+\sigma)-2n^2(1+2\sigma+\sigma^2)+2n\sigma(1+\sigma)-\sigma^2]}{[1-a(-\sigma+2n(1+\sigma)-3n^2)]^3},$$

and the speed is given by Eq. (29). Figure 4 shows the lower and upper bounds for $a=1/2$, as well as the speed obtained from numerical simulations of Eqs. (4) and (33). According to Fig. 4, the upper bound from the variational method is better than the bound $c_{\max}=1/\sqrt{a}=\sqrt{2}$, which has been discussed previously in the context of bistable systems [11]. It is worth noting that in this case there is excellent agreement between the lower bound we have been able to derive and the numerical solution. In Fig. 4 we also observe the change of sign for the speed at $\sigma=1/2$. The restriction for the validity of the variational method $a<M^{-1}$ for $M=\max_{n\in(0,1)}f'(n)$ yields to $a<3/(\sigma^2-\sigma+1)$, which imposes no additional restriction for $a=1/2$.

V. TIME-DELAYED LOTKA-VOLTERRA EQUATIONS

In this section we consider a system with two variables n and m undergoing reaction-diffusion dynamics. In biological applications, they may represent the predator and prey species [22], the farmers and hunter-gatherers in the expansion of agricultural communities [21], the infected and susceptible individuals in the spread of a pandemic [20], etc. Such systems of equations are called Lotka-Volterra equations. Two-variable systems are also important in the propagation of domain walls in superconductors; here n corresponds to the superconducting order parameter, m to the gauge-invariant vector potential and they follow Ginzburg-Landau equations [27] which have in fact the same mathematical form of Lotka-Volterra equations.

A. General theory

Let us consider the system

$$\begin{aligned}\tau n_{tt}+n_t&=Dn_{xx}+F(n)+\tau F'(n)n_t+\gamma nm,\\ \hat{\tau}m_{tt}+m_t&=\hat{D}m_{xx}+\hat{F}(m)+\hat{\tau}\hat{F}'(m)n_t-\hat{\gamma}nm,\end{aligned} \tag{34}$$

which is a pair of coupled HRD equations [see Eq. (3)]. The superscript $\hat{}$ refers to the species with number density m, and the last term in these equations corresponds to the interaction between both species. This simple term means that in, e.g., a predator-prey system with $\tau=\hat{\tau}=0$, the predators increase their population density n because of their interaction with preys, which in turn experience a decrease in their popula-

tion density m. It should be emphasized that here we are assuming that the interaction rate γnm is small compared to the other terms, since otherwise higher-order terms in n^2m, etc. could be important in the description of the interaction among both species. For $\tau=\hat{\tau}=0$ we recover the usual (or PRD) Lotka-Volterra system with spatial inhomogeneities (see Chap. 12 in Ref. [22]). Wave-front solutions to Eqs. (34) have not been reported up to now in the literature, to our knowledge. Here we shall tackle this problem by extending the theory presented in Secs. II and III. As said above, we consider HRD equations, thus the results applying to PRD equations will follow in the limit $\tau\to 0$. In order to illustrate our procedure, let us consider for a moment a specific problem: in the Neolithic transition, the population wave fronts of farmers (with number density n) traveled into areas where they encountered a population of preexisting hunter-gatherers with a number density m that is usually assumed to be approximately uniform, say m_0 [21,40]. Both populations mixed to some extent, and this interaction is regarded as the cause of the gradients observed in the present spatial distribution of human genes [21]. We may describe the process by following exactly the same procedure as in Sec. II but making use of the coupled Eqs. (34) instead of Eq. (3): the procedure is essentially the same as in Sec. II, so we shall only give the main steps. Since the problem we have in mind is the expansion of, say, farming communities, we consider the corresponding equation in the leading edge of the front ($n\approx 0$),

$$(1-ac^2)\epsilon_{zz}+c[1-af'(0)]\epsilon_z+[f'(0)+\tilde{\gamma}m_0]\epsilon=0, \tag{35}$$

where $\tilde{\gamma}=\gamma/k$, and the rest of the notation is the same as in Sec. II. This equation generalizes Eq. (6) and is decoupled from the evolution equation of species m. Note that we cannot apply Eq. (9) with $f'(0)+\gamma m_0$ instead of $f'(0)$, because the parentheses multiplying ϵ_z in Eq. (35) does not contain $f'(0)+\gamma m_0$ but only $f'(0)$, thus Eq. (35) does not have the same form as Eq. (6). But it is clear that, as in Sec. II, the asymptotic solutions near $n=0$ are given by Eq. (8), with $\lambda_\pm$ the solution to the characteristic equation, which now reads

$$(1-ac^2)\lambda^2+c[1-af'(0)]\lambda+f'(0)+\tilde{\gamma}m_0=0. \tag{36}$$

As in Sec. II, we require $\mathrm{Im}(\lambda)=0$ in order to prevent the solution from oscillating. This yields

$$c\geq 2\sqrt{\frac{f'(0)+\tilde{\gamma}m_0}{[1+af'(0)]^2+4a\tilde{\gamma}m_0}}. \tag{37}$$

This result reduces, as it should, to the lower bound (9) for noninteracting species ($\tilde{\gamma}=0$). On the other hand, in the absence of a delay time τ (i.e., $a=\tau k=0$) we obtain

$$c\geq 2\sqrt{f'(0)+\tilde{\gamma}m_0}, \tag{38}$$

and if we assume that both the effect of the interaction and that of the delay are negligible we recover Fisher's result for PRD equations, namely $c\geq 2\sqrt{f'(0)}$. Equation (38) could have been obtained simply from the fact that in the nondelayed (or PRD) model $\tau=0$, the first Eq. (34) is nothing but a PRD equation with $f(n)+\gamma nm$ instead of $f(n)$, and we have assumed that $m\approx m_0$ near $n=0$. The PRD limit (38) agrees with previous research, where it has been applied to predator-prey systems [41] and to the propagation of interfaces in superconductors [42].

It should be noted that Eq. (37) provides just a lower bound, simply because it is based on the linear approach (Sec. II). We now make use of our variational approach to HRD Eqs. (Sec. III). First of all we note that we cannot make use of Eq. (30) with $f'(0)+\gamma m_0$ instead of $f'(0)$, because the evolution equation corresponding to the first Eq. (34) is

$$(1-ac^2)n_{zz}+c[1-af'(n)]n_z+f(n)+\tilde{\gamma}m_0n=0, \tag{39}$$

and this is not reducible to an equation such as Eq. (5), since $[f(n)+\tilde{\gamma}m_0n]'=f'(n)+\tilde{\gamma}m_0\neq f'(n)$. Thus we have to generalize the approach in Sec. III. Since the steps are exactly the same as there, it will suffice to sketch the derivation. Equation (15) is generalized into

$$(1-ac^2)p\frac{dp}{dn}-c[1-af'(n)]p+f(n)+\tilde{\gamma}m_0n=0. \tag{40}$$

We multiply this by g/p, with $p\equiv -n_z$ and $g>0$, and integrate by parts. As before, $h=-g'>0$ and we apply the general inequality $(r+s)\geq 2\sqrt{rs}$ to get rid of p. This finally yields

$$\frac{c}{\sqrt{1-ac^2}}\geq 2\frac{\int_0^1\sqrt{[f(n)+\tilde{\gamma}m_0n]gh}\,dn}{\int_0^1 g[1-af'(n)]dn}, \tag{41}$$

which generalizes Eq. (18).

We can now derive lower and upper bounds from the variational analysis. If we consider again the trial functions $g=n^{\alpha-1}$, Eq. (41) becomes

$$\frac{c}{\sqrt{1-ac^2}}\geq 2\sqrt{1-\alpha}\frac{\int_0^1 n^{\alpha-3/2}\sqrt{[f(n)+\tilde{\gamma}m_0n]}\,dn}{\int_0^1 n^{\alpha-1}[1-af'(n)]dn}.$$

In the limit $\alpha\to 0$, the integrands diverge at $n=0$, as in Sec. III, thus only the singular point will contribute. We expand the integrands in Taylor series near $n=0$, and only the leading term in the expansions will survive. Thus, assuming $f'(0)\neq 0$,

$$\frac{c}{\sqrt{1-ac^2}}\geq 2\sqrt{1-\alpha}\frac{\int_0^\varepsilon n^{\alpha-3/2}\sqrt{f'(0)n+\tilde{\gamma}m_0}\,dn}{\int_0^\varepsilon n^{\alpha-1}[1-af'(0)]dn}.$$

Performing the integrals and taking the limit $\alpha\to 0$ we obtain

$$c \geqslant c_L = 2\sqrt{\frac{f'(0)+\tilde{\gamma}m_0}{[1+af'(0)]^2+4a\tilde{\gamma}m_0}}, \tag{42}$$

in agreement with the result (37) from the linear analysis. Thus also for interacting species, the linearization and variational methods yield the same lower bound. We now derive upper bounds. Since the only change of Eq. (41) relative to Eq. (18) is that $f+\tilde{\gamma}m_0 n$ appears instead of f, we define $\mu(n)$ and $\alpha(n)$ performing this change in the corresponding definitions in Sec. III B, i.e., $\mu(n)=g[1-af']$ as before and $\alpha(n)=(f+\tilde{\gamma}m_0 n)h/[g(1-af')^2]$. We have then, from Eqs. (41) and (23),

$$\frac{c}{\sqrt{1-ac^2}} \leqslant 2\max_g \left[\frac{\int_0^1 \frac{(f+\tilde{\gamma}m_0 n)h}{1-af'}dn}{\int_0^1 g(1-af')dn} \right]^{1/2}.$$

We integrate by parts,

$$\int_0^1 \frac{(f+\tilde{\gamma}m_0 n)h}{1-af'}dn = -\frac{g(1)\tilde{\gamma}m_0}{1-af'(1)} + \int_0^1 g\left(\frac{f'+\tilde{\gamma}m_0}{(1-af')^2} + \frac{af''(f+\tilde{\gamma}m_0 n)}{(1-af')^3} \right) dn. \tag{43}$$

We note that, in contrast to what happened in the case of a single species [Eq. (25)], the boundary term does not vanish. But recalling that $g>0$ and the condition $1-af'>0$, we have

$$\int_0^1 \frac{(f+\tilde{\gamma}m_0 n)h}{1-af'}dn \leqslant \int_0^1 g\left(\frac{f'+\tilde{\gamma}m_0}{(1-af')^2} + \frac{af''(f+\tilde{\gamma}m_0 n)}{(1-af')^3} \right) dn,$$

and, in order to get an upper bound independent of g,

$$\int_0^1 \frac{(f+\tilde{\gamma}m_0 n)h}{1-af'}dn \leqslant \sup_{n\in(0,1)} \left[\frac{f'+\tilde{\gamma}m_0}{(1-af')^2} + \frac{af''(f+\tilde{\gamma}m_0 n)}{(1-af')^3} \right] \int_0^1 g(1-af')dn. \tag{44}$$

Thus,

$$\Phi(n) \equiv \frac{f'+\tilde{\gamma}m_0}{(1-af')^2} + \frac{af''(f+\tilde{\gamma}m_0 n)}{(1-af')^3}. \tag{45}$$

As in Sec. III B, if we assume that the source function f is continuous and concave and recall again the condition $1-af'>0$, we see that the second term in $\Phi(n)$ is negative (it only vanishes at $n=0,1$), whereas the first term decreases for increasing values of n. Thus,

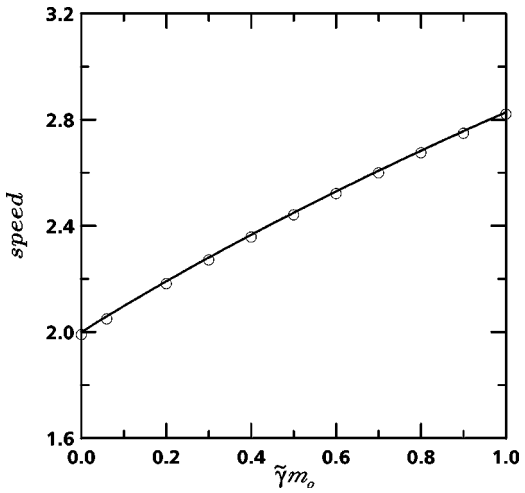

FIG. 5. Comparison between analytical results and numerical simulations for the dimensionless front speed in PRD Lotka-Volterra equations, as a function of the interaction parameter $\tilde{\gamma}m_0$. The dots are results from numerical simulations of Eqs. (49) for the PRD case ($\tau=0$) and $f'(0)=1$. The solid line is the prediction given by Eq. (48).

$$\sup_{n\in(0,1)} \Phi(n) = \frac{f'(0)+\tilde{\gamma}m_0}{[1-af'(0)]^2},$$

and we have the simpler result

$$c \leqslant c_U = 2\sqrt{\frac{f'(0)+\tilde{\gamma}m_0}{[1+af'(0)]^2+4a\tilde{\gamma}m_0}}, \tag{46}$$

which reduces to Eq. (30) in the limit $\tilde{\gamma}\to 0$, as it should, and holds provided that f is continuous and concave in (0,1). Under these assumptions, our upper bound is the same as the lower one Eq. (42), and the asymptotic speed of the fronts for interacting species can also be predicted without any uncertainty

$$c = 2\sqrt{\frac{f'(0)+\tilde{\gamma}m_0}{[1+af'(0)]^2+4a\tilde{\gamma}m_0}}. \tag{47}$$

If the delay time is not taken into account (PRD approach, $a=0$), this reduces to

$$c = 2\sqrt{f'(0)+\tilde{\gamma}m_0}, \tag{48}$$

in agreement to previous work [41,42]. In Fig. 5 we compare this analytical result for the expansion of species n with those obtained from numerical simulations for the case $\tau=0$. The numerical simulations have been performed by assuming that initially $n=1$ in a localized region and $n=0$ elsewhere (as in Figs. 1–4) and $m=m_0$ everywhere; the equations used are Eq. (34) in the same variables as Eq. (4), i.e.,

$$an_{tt}+n_t = n_{xx}+f(n)+af'(n)n_t+\tilde{\gamma}nm_0, \tag{49}$$

$$\hat{a}m_{tt}+m_t = m_{xx}+\hat{f}(m)+\hat{a}\hat{f}'(m)m_t+\hat{\tilde{\gamma}}nm_0,$$

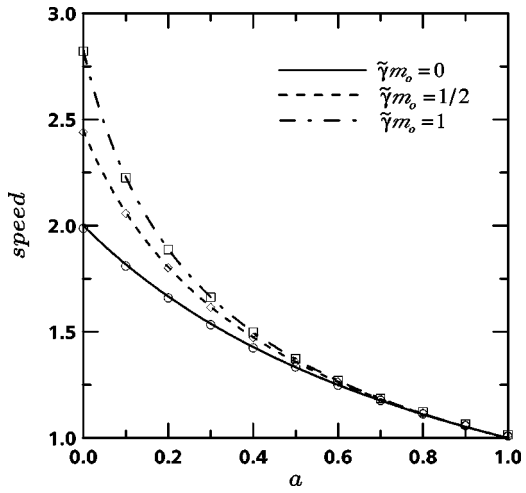

FIG. 6. Comparison between analytical results and numerical simulations for the dimensionless front speed in HRD (or time-delayed) Lotka-Volterra equations, as a function of a (for $\tilde{\gamma}m_0 = 0,1/2,1$). The symbols are results from numerical simulations of Eqs. (49), and the solid lines are the predictions from Eq. (47). There is excellent agreement in all cases.

where $\hat{a} = \hat{k}\hat{\tau}$, $\hat{\tilde{\gamma}} = \tilde{\gamma}/\hat{k}$ and, analogously to Eq. (4), $1/\hat{k}$ is a characteristic reactive time for species m. In the simulations we have assumed for definiteness that $\hat{a} = a, \hat{\tilde{\gamma}} = \hat{\gamma}$, as well as logistic growth functions, i.e., $f(n) = n(1-n)$ and $\hat{f}(m) = m(1-m)$. In Fig. 6 we compare the predictions of Eq. (47) to the simulations of Eqs. (49) for $\tau \neq 0$. There is good agreement in both the classical (Fig. 5) and the time-delayed (Fig. 6) cases. By comparison to the results for $\gamma m_0 = 0$, it is also seen that the interaction among both species leads to a faster wave front, as was to be expected since the last term in the first Eq. (34) corresponds to a numeric increase in the expanding species. This was conjectured in Ref. [12] and is why the front speed increases with increasing values of $\tilde{\gamma}m_0$.

It had been pointed out [17] that a variational characterization for a system such as Eq. (34) (even in the PRD case) was an important problem that remained to be studied. Here we have presented a solution to this problem both for PRD and HRD equations.

B. Application to the Neolithic transition

Finally, we apply the results for interacting species to the waves of advance of farming populations in the Neolithic transition. We already considered this problem in our previous paper [12], but did not take into account the interaction between the expanding farmers and the preexisting hunter-gatherers. This interaction is important, as mentioned in Sec. V A, because it is thought to have caused the genetic clines (or gradients) observed in human populations across Europe and Asia [21]. This is why the two-species model has been proposed for this expansion [21,40], although no analytical results have been previously derived. Recalling that in Sec. II we have introduced dimensionless variables, the speed of the front v is related to the dimensionless speed c through $v = \sqrt{Dk}c$. We also recall that we have introduced $a = \tau k$, $f(n) = F(n)/k$ and $\tilde{\gamma} = \gamma/k$. From Eq. (47) we have two cases for interacting populations:

(i) *PRD approach:* it is based on the assumption that the role of the delay time can be neglected ($\tau \approx 0$). Then we have from Eq. (48)

$$v_{\mathrm{PRD}} = 2\sqrt{D[F'(0) + \gamma m_0]}, \tag{50}$$

which becomes Fisher's result $2\sqrt{DF'(0)}$ for noninteracting species, as it should.

(ii) *HRD approach:* it takes the delay time τ into account. Then Eq. (47) applies

$$v_{\mathrm{HRD}} = \frac{2\sqrt{D[F'(0) + \gamma m_0]}}{\sqrt{[1 + \tau F'(0)]^2 + 4\tau\gamma m_0}}. \tag{51}$$

In spite of the fact that the Neolithic transition took place in two dimensions, our one-dimensional results are still valid. This can be seen from the fact that in two-dimensions, the only change in Eqs. (34) is that we have $\nabla^2 n$ instead of n_{xx} (and $\nabla^2 m$ instead of m_{xx}). However, in polar coordinates $\nabla^2 n = \partial^2/\partial r^2 + 1/r\ \partial n/\partial r \to \partial^2/\partial r^2$ as $r \to \infty$, which corresponds to the asymptotic front [43]: it is the propagation of this front that we are interested in (we have assumed, as usual, [43], that n is independent of the polar angle θ).

In order to obtain numerical values for both speeds (50) and (51) we need values for the parameters appropriate to the Neolithic transition. As explained in Ref. [12], such values have been derived from observations independent of the Neolithic expansion and their mean values are $F'(0) = 0.032\ \mathrm{yr}^{-1}$, $D = 15.44\ \mathrm{km}^2/\mathrm{yr}$ and $\tau = 12.5$ yr (the latter value follows from the mean generation time) [44]. On the other hand, from the observations in Ref. [40] we have the mean values for the other two parameters $m_0 = 0.04$ hunters/km and $\gamma = 5.84\ \mathrm{km}^2/(\text{hunter yr})$ [45]. Use of these values in Eq. (50) yields $v_{\mathrm{PRD}} = 1.6$ km/yr, which is much higher than the speed derived from the archaeological record; in contrast Eq. (51) yields $v_{\mathrm{HRD}} = 1.1$ km/yr, which lies entirely within the experimental range, namely 1.0 ± 0.2 km/yr (see the text as well as Fig. 1 in Ref. [12]). This is a strong point for the applicability of HRD equations to human populations, and seems to indicate that HRD equations could become very important in the understanding of the range dynamics of biological species. In Ref. [12], we showed that when the interaction among populations is not taken into account, an HRD approach gives better results for the Neolithic transition than the usual, PRD approach. Here we have shown that this conclusion remains valid if the effect of the interaction among farmers and hunter-gatherers is not neglected.

VI. CONCLUSIONS

In this work we have performed numerical and analytical analyses on the front speed problem in hyperbolic reaction-diffusion equations. We have made use of two analytical techniques. First, a linear analysis near the equilibrium points of the systems. Second, we have used and generalized a recent variational analysis derived by Benguria and Depassier [16] for PRD equations. It is a very useful method for HRD equations also. The general form of this method takes

into account the nonlinear effects of the source term, and lower and upper bounds have been obtained. We have analyzed the application of this method to several systems of biological interest. For logistic and generalized Fisher-Kolmogorov kinetics, linear and nonlinear analysis yield the same results, the selected speed may be obtained exactly and coincides with that obtained from linear analysis and with numerical results. For forest fire models, linear analysis does not hold and the variational method becomes especially useful since a new, improved upper bound has been obtained. We have found lower and upper bounds and the numerical value for the speed of fire fronts. Both bounds and the numerical solution for the speed are decreasing function with increasing β as is expected in forest fire models. Also for a cubic source term and for bistable systems, analytical and numerical results are in agreement. We have also extended our model to a system of two reaction-diffusing equations, the so-called Lotka-Volterra equations but incorporating a delay time. Results are again in agreement with simulations, and we have obtained estimations that are consistent with the available experimental measurements for the spread of farming communities in the Neolithic transition.

ACKNOWLEDGMENTS

The authors would like to thank Professor Casas-Vázquez for discussions. This work has been partially funded by the DGICYT of the Ministry of Education and Culture under Grant No. PB 96-0451 (J.F.).

[1] D.G. Aronson and H.F. Weinberger, Adv. Math. **30**, 33 (1978).
[2] G. Dee and J.S. Langer, Phys. Rev. Lett. **50**, 383 (1978).
[3] L. Chen, N. Goldenfeld, and Y. Oono, Phys. Rev. E **49**, 4502 (1994).
[4] E. Ben-Jacob, H.R. Brand, G. Dee, L. Kramer, and J.S. Langer, Physica D **14**, 348 (1985).
[5] G.I. Taylor, Proc. London Math. Soc. **20**, 196 (1921).
[6] H.D. Weyman, Am. J. Phys. **35**, 488 (1965).
[7] D. Jou, J. Casas-Vázquez, and G. Lebon, *Extended Irreversible Thermodynamics* (Springer, Berlin, 1996).
[8] K.P. Hadeler, Can. Appl. Math. Quart. **2**, 27 (1994).
[9] V. Méndez and J. Camacho, Phys. Rev. E **55**, 6476 (1997).
[10] V. Méndez and J.E. Llebot, Phys. Rev. E **56**, 6557 (1997).
[11] V. Méndez and A. Compte, Physica A **260**, 90 (1998).
[12] J. Fort and V. Méndez, Phys. Rev. Lett. **82**, 867 (1999).
[13] J. Fort, J. Casas-Vázquez, and V. Méndez, J. Phys. Chem. B **103**, 860 (1999).
[14] A. J. Lotka, *Elements of Mathematical Biology* (Dover, New York, 1956).
[15] W. van Saarloos, Phys. Rev. A **37**, 211 (1988).
[16] R.D. Benguria and M.C. Depassier, Phys. Rev. E **57**, 6493 (1998).
[17] R.D. Benguria and M.C. Depassier, Phys. Rev. Lett. **73**, 2272 (1994); **77**, 1171 (1996); Commun. Math. Phys. **175**, 221 (1996).
[18] S. Gradshteyn and I. M. Ryzhik, *Table of Integrals, Series and Products* (Academic, San Diego, 1994), p. 1133, formula HL151 (see also note [13] in Ref. [16]).
[19] A. N. Kolmogorov, I. G. Petrovskii, and N. S. Piskunov, in *Selected works of A. M. Kolmogorov*, edited by V. M. Tikhomirov (Kluwer, Amsterdam, 1991).
[20] R.A. Fisher, Ann. Eugenics **7**, 355 (1937).
[21] A.J. Ammerman and L.L. Cavalli-Sforza, *The Neolithic Transition and the Genetics of Population in Europe* (Princeton University Press, Princeton, 1984).
[22] J.D. Murray, *Mathematical Biology* (Springer-Verlag, Berlin, 1993).
[23] J.V. Noble, Nature (London) **250**, 726 (1974).
[24] J. Engelbrecht, Proc. R. Soc. London, Ser. A **375**, 195 (1981).
[25] A.B. Feldman, Y.B. Chernyak, and R.J. Cohen, Phys. Rev. E **57**, 7025 (1998).
[26] N. Barkai, M.D. Rose, and N.S. Wingeen, Nature (London) **396**, 422 (1998).
[27] S.J. Di Bartolo and A.T. Dorsey, Phys. Rev. Lett. **77**, 4442 (1996).
[28] A.A. Wheeler, W.J. Boettinger, and G.B. McFadden, Phys. Rev. A **45**, 7424 (1992).
[29] W. van Saarloos, M. van Hecke, and R. Holyst, Phys. Rev. E **52**, 1773 (1995).
[30] A. Lemarchand and B. Nowakowski, J. Chem. Phys. **109**, 7028 (1998).
[31] T. Dedeurwaerdere, J. Casas-Vázquez, D. Jou, and G. Lebon, Phys. Rev. E **53**, 498 (1996).
[32] S. Fedotov, Phys. Rev. E **58**, 5143 (1998).
[33] W.H. Press, S.A. Teukolsky, W.T. Vetterling, and B.P. Flannery, *Numerical Recipes* (Cambridge University Press, Cambridge, 1992).
[34] K.P. Hadeler and F. Rothe, J. Math. Biol. **2**, 251 (1975).
[35] M.A. Livshits, G.T. Gurija, B.N. Belinstev, and M.V. Volkenstein, J. Math. Biol. **11**, 295 (1981); see also E. Magyari, J. Phys. A **15**, L139 (1982).
[36] H.M. Lieberstein, Math. Biosci. **1**, 45 (1967); H.P. McKean, Adv. Math. **4**, 209 (1970).
[37] G. Izús, R. Deza, O. Ramírez, H.S. Wio, D.H. Zanette, and C. Borzi, Phys. Rev. E **52**, 129 (1995).
[38] A.S. Mikhailov, *Foundations of Synergetics I* (Springer-Verlag, Berlin, 1990).
[39] J.D. Murray, *Mathematical Biology* (Springer-Verlag, Berlin, 1989).
[40] S. Rendine, A. Piazza, and L.L. Cavalli-Sforza, Am. Nat. **128**, 681 (1986).
[41] J. D. Murray, *Mathematical Biology* (Ref. [22]), Eq. (12.10). See also S.R. Dunbar, J. Math. Biol. **17**, 11 (1983); Trans. Am. Math. Soc. **268**, 557 (1984).
[42] Ref. [27], Eq. (7). Note the different units and the minus sign in that equation, which arise because of the minus sign in the term $-q^2 f$ in Eq. (2). In this reference q^2, Q_∞^2, and f correspond to $\tilde{\gamma}m$, $\tilde{\gamma}m_0$, and n here, respectively, and we have considered the case of small reduced interaction rate $\tilde{\gamma}m_0$ (small values of Q_∞^2 in Ref. [27]). Otherwise the interaction rate would be fast enough to modify m and n in very short time scales, thus the approximation $m \approx m_0$ would break down even in the leading edge of the front (i.e., near $n=0$).

[43] See J. D. Murray, *Mathematical Biology* (Ref. [22]), p. 281.

[44] See Fig. 2 and Eq. (12) in Ref. [12]. That equation applies to diffusion in two-dimensional space. On the other hand, according to the notation in the present paper τ corresponds to $\tau/2$ in Ref. [12] [compare Eq. (3) in the present paper and Eq. (7) in Ref. [12]].

[45] Note the units used in Ref. [40]: $\gamma = 0.0024$ (tribe area)/(hunter generation)$\cdot$(156 km)^2/ (tribe area)$\cdot$1 generation/25 yr$=0.23$ km^2/(hunter yr).